CHAPTER 5

Examination Mammogram Images using FCOM texture features

This chapter reports the results of abnormalities mammogram images detection system [49 - 50]. We developed a detection system without any mammogram preprocessing for four breast abnormalities factors in Breast Imaging-Reporting and Data System (BI-RADS) [51], i.e. calcification (CALC), well-defined/circumscribed masses (CIRC), spiculated masses (SPIC), and architectural distortion (ARCH). A Fuzzy Co-Occurrence Matrix (FCOM) is employed to create a feature sets and then a Support Vector Machine (SVM) is executed as the classifier. To give a comparison, we also created a feature sets extracted from a regular Gray Level Co-occurrence Matrix (GLCM). This chapter is organized in three section. Section 5.1 describes the proposed breast abnormalities detection system. Then, the detection results and discussions are presented in section 5.2. Finally, the summary of this chapter is given in section 5.3.

5.1 Experimental design

The experiment consists of 2 parts, i.e., training phase and testing phase as shown in figure 5.1. In training process, the RBF σ was set to 0.1, 0.25, 0.5, 0.75, 1.0, 1.5, 2.0, 2.5, 3.0, 3.5, 4.0, 4.5, 5.0, 10.0, 20.0, 30.0, 40.0, and 50.0. We also implemented 7-fold cross validation in the experiment to give the generalized information of the system. For testing process, we selected the best validation set detection model to evaluate the performance of our system.

For feature extraction, we utilized FCM with C = 4 and 8 in order to generate the texture feature from the FCOM. To compute FCOM, we were setting d = 1. Then, we computed 4 of 14 features, i.e., the contrast, correlation, energy, and homogeneity for one direction (θ = 0°). This generated a feature set called FzCM1. For four directions (θ = 0°, 45°, 90°, and 135°), they generated a feature set called FzCM2. We also

calculated the average and standard deviation from each feature from all directions called FzCM3.

For fourteen features in one direction, they generated a feature set called FzCM4. For four directions, we call them as FzCM5. Next, we created FzCM6 from the average and standard deviation of all directions from FzCM5. Similar to FCOM, we also generated feature sets for GLCM with the same conditions namely GLCM1, GLCM2, GLCM3, GLCM4, GLCM5, and GLCM6, respectively. The comparison between FCOM and GLCM feature sets are shown in table 5.1. The testing results of FCOM and GLCM are compared for evaluating their performances. In addition, we reduced the dimension by using principal component analysis (PCA). Moreover, each feature dimension was normalized using (4.1)

To evaluate the detection performance, we computed the accuracy (ACC), the likelihood of detecting abnormalities, and false alarm per image (FPI) using

$$\mathrm{ACC} = \left(\frac{1}{\#\ \text{Number of all ROIs}} \right) \times \#\ \text{Number of all TP from blind testing image}, \quad (5.1)$$

$$\mathrm{FPI} = \frac{\#\ \text{Number of all FP from all blind testing images}}{\#\ \text{Number of all blind testing images}}, \quad (5.2)$$

where ROIs is the number of all abnormalities from blind testing images (ground truth).

Table 5.1 The mammogram image textural feature sets comparison.

FCOM			**GLCM**		
Feature set name	**Feature dimensions**		**Feature set name**	**Feature dimensions**	
	Non PCA	PCA		Non PCA	PCA
FzCM1	4×*C*	4	GLCM1	4	4
FzCM2	16×*C*	16	GLCM2	16	16
FzCM3	8×*C*	8	GLCM3	8	8
FzCM4	14×*C*	4	GLCM4	14	4
FzCM5	56×*C*	16	GLCM5	56	16
FzCM6	28×*C*	8	GLCM6	28	8

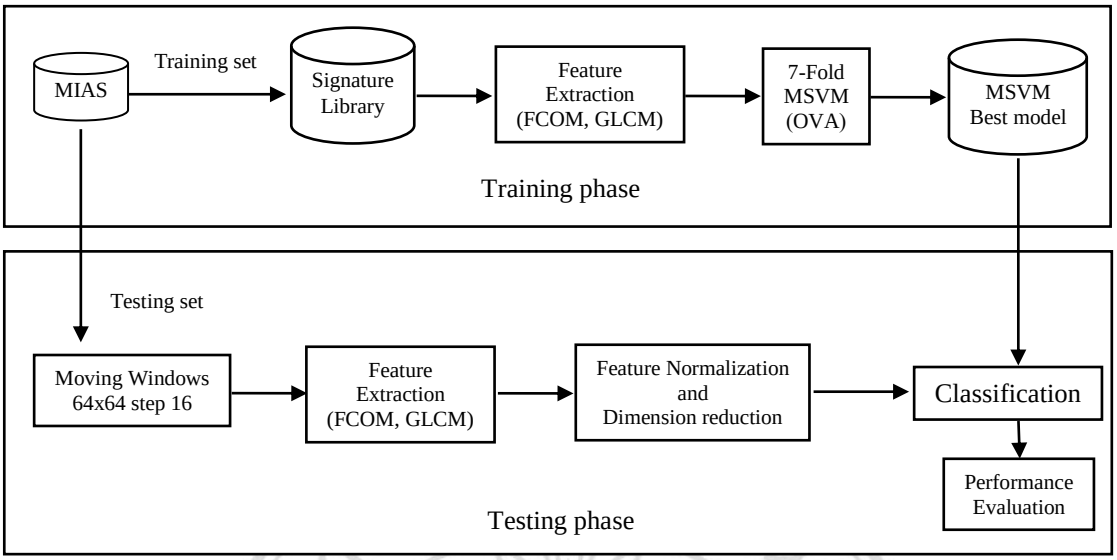

Figure 5.1 Abnormalities mammogram image detection system.

5.2 Detection results and discussions

The experiments were test on the standard data set from Mammographic Image Analysis Society, called mini-MIAS data set (The Mammographic Images Analysis Society) [52 - 53]. There were 322 mammograms with the size of 1024×1024 containing 7 classes, i.e., architectural distortion (ARCH), asymmetry (ASYM), calcification (CALC), circumscribed masses (CIRC), other ill-defined masses (MISC), spiculated mass (SPIC), and normal (NORM). In our experiment, we did not use mammograms from ASYM and MISC classes because of several varieties of shapes in these 2 classes. Moreover, the number of samples in MISC class was limited. Also, in the real world diagnosis, it was known that ASYM class was associated with several abnormalities, e.g., AD and CALC.

In training task, we selected 75 mammograms, i.e., 42 NORM, 6 CALC, 8 CIRC, 10 ARCH, and 9 SPIC mammograms to be our training data set. For each mammogram in the training data set, we manually selected images with the size of 64×64 and collected them in a signature library. Hence, we had 42 NORM, 21 CALC, 21 CIRC, 42 ARCH, and 42 SPIC sub-images in the signature library. The examples of sub-images in the signature library are shown in figure 5.2. The remaining 218 mammograms, i.e., 167 NORM, 17 CALC, 15 CIRC, 9 ARCH, and 10 SPIC mammograms were used as the

blind test set. The summary of mammogram images used in this experiment is shown in table 5.2.

(a) CALC (b) CIRC (c) SPIC (d) ARCH (e) NORM

Figure 5.2 An example of sub-images in the signature library.

Table 5.2 Summary of mammogram images data set.

Abnormal mammogram type	No. of Samples		
	Training images	Training data set	Testing images
CALC	6	21	17
CIRC	8	21	15
SPIC	9	42	10
ARCH	10	42	9
NORM	42	42	167
Total	75	168	218

From the training data set, the best validation set detection results from FCOM are shown in table 5.3. The confusion matrices from these results are presented in table 5.4 to 5.15. Table 5.16 shows the best validation set detection results from GLCM feature sets. Similarly, the confusion matrices from GLCM detection results are shown in table 5.17 to 5.28. We found that the highest correct classification result from FzCM6 at 4 clusters was 100%. The second highest correct classification result was 95.83% at FzCM3 from 4 clusters, FzCM2 and FzCM6 from 8 clusters. There was GLCM6 at 8 gray levels that yielded 100% correct classification. The second best validation set result, i.e. 95.83% correct classification, was from GLCM4 at 8 gray levels. The best results confusion matrices of each experimental set are shown in the following table.

Table 5.3 The best validation set detection results from FCOM feature sets.

C	Feature set	non PCA		PCA	
		RBF (σ)	ACC (%)	RBF (σ)	ACC (%)
4	FzCM1	0.75	83.33	2.00	75.00
	FzCM2	1.50	87.50	3.00	91.67
	FzCM3	3.00	95.83	3.50	91.67
	FzCM4	2.00	87.50	2.00	70.83
	FzCM5	4.00	91.67	4.00	91.67
	FzCM6	5.00	100.00	4.00	83.33
8	FzCM1	1.50	83.33	4.00	87.50
	FzCM2	4.50	95.83	30.00	70.83
	FzCM3	3.00	91.67	10.00	87.50
	FzCM4	3.00	87.50	10.00	70.83
	FzCM5	5.00	87.50	3.00	79.19
	FzCM6	5.00	95.83	3.00	95.83

Table 5.4 The best validation set detection result confusion matrices from FzCM1 at $C = 4$.

without PCA

Program output \ Desired output	ARCH	SPIC	CALC	CIRC	NORM
ARCH	5	0	0	0	1
SPIC	1	4	0	1	0
CALC	0	0	2	0	1
CIRC	0	0	0	3	0
NORM	0	0	0	0	6

with PCA

Program output \ Desired output	ARCH	SPIC	CALC	CIRC	NORM
ARCH	4	1	0	0	1
SPIC	2	3	0	1	0
CALC	1	0	2	0	0
CIRC	0	0	0	3	0
NORM	0	0	0	0	6

Table 5.5 The best validation set detection result confusion matrices from FzCM2 at $C = 4$.

without PCA

Program output \ Desired output	ARCH	SPIC	CALC	CIRC	NORM
ARCH	5	1	0	0	0
SPIC	0	5	1	0	0
CALC	0	0	3	0	0
CIRC	0	0	0	3	0
NORM	0	1	0	0	5

with PCA

Program output \ Desired output	ARCH	SPIC	CALC	CIRC	NORM
ARCH	6	0	0	0	0
SPIC	0	6	0	0	0
CALC	0	1	1	0	1
CIRC	0	0	0	3	0
NORM	0	0	0	0	6

Table 5.6 The best validation set detection result confusion matrices from FzCM3 at $C = 4$.

without PCA

Program output \ Desired output	ARCH	SPIC	CALC	CIRC	NORM
ARCH	6	0	0	0	0
SPIC	1	5	0	0	0
CALC	0	0	3	0	0
CIRC	0	0	0	3	0
NORM	0	0	0	0	6

with PCA

Program output \ Desired output	ARCH	SPIC	CALC	CIRC	NORM
ARCH	6	0	0	0	0
SPIC	0	6	0	0	0
CALC	0	0	1	0	2
CIRC	0	0	0	3	0
NORM	0	0	0	0	6

Table 5.7 The best validation set detection result confusion matrices from FzCM4 at $C = 4$.

without PCA

Program output \ Desired output	ARCH	SPIC	CALC	CIRC	NORM
ARCH	6	0	0	0	0
SPIC	0	6	0	0	0
CALC	1	0	1	1	0
CIRC	0	0	0	3	0
NORM	1	0	0	0	5

with PCA

Program output \ Desired output	ARCH	SPIC	CALC	CIRC	NORM
ARCH	3	3	0	0	0
SPIC	0	4	1	1	0
CALC	0	1	2	0	0
CIRC	0	1	0	2	0
NORM	0	0	0	0	6

Table 5.8 The best validation set detection result confusion matrices from FzCM5 at $C = 4$.

without PCA

Program output \ Desired output	ARCH	SPIC	CALC	CIRC	NORM
ARCH	5	0	0	0	1
SPIC	0	6	0	0	0
CALC	0	0	3	0	0
CIRC	0	0	0	3	0
NORM	0	0	1	0	5

with PCA

Program output \ Desired output	ARCH	SPIC	CALC	CIRC	NORM
ARCH	6	0	0	0	0
SPIC	0	4	1	1	0
CALC	0	0	3	0	0
CIRC	0	0	0	3	0
NORM	0	0	0	0	6

Table 5.9 The best validation set detection result confusion matrices from FzCM6 at $C = 4$.

without PCA

Program output \ Desired output	ARCH	SPIC	CALC	CIRC	NORM
ARCH	6	0	0	0	0
SPIC	0	6	0	0	0
CALC	0	0	3	0	0
CIRC	0	0	0	3	0
NORM	0	0	0	0	6

with PCA

Program output \ Desired output	ARCH	SPIC	CALC	CIRC	NORM
ARCH	4	1	0	0	1
SPIC	0	5	0	1	0
CALC	0	1	2	0	0
CIRC	0	0	0	3	0
NORM	0	0	0	0	6

Table 5.10 The best validation set detection result confusion matrices from FzCM1 at $C = 8$.

without PCA

Program output \ Desired output	ARCH	SPIC	CALC	CIRC	NORM
ARCH	6	0	0	0	0
SPIC	1	5	0	0	0
CALC	0	0	1	0	2
CIRC	0	0	0	3	0
NORM	1	0	0	0	5

with PCA

Program output \ Desired output	ARCH	SPIC	CALC	CIRC	NORM
ARCH	5	0	0	0	1
SPIC	0	6	0	0	0
CALC	0	0	3	0	0
CIRC	0	1	0	2	0
NORM	1	0	0	0	5

Table 5.11 The best validation set detection result confusion matrices from FzCM2 at $C = 8$.

without PCA

Program output \ Desired output	ARCH	SPIC	CALC	CIRC	NORM
ARCH	6	0	0	0	0
SPIC	0	6	0	0	0
CALC	1	0	2	0	0
CIRC	0	0	0	3	0
NORM	0	0	0	0	6

with PCA

Program output \ Desired output	ARCH	SPIC	CALC	CIRC	NORM
ARCH	6	0	0	0	0
SPIC	1	5	0	0	0
CALC	2	1	0	0	0
CIRC	2	0	0	0	1
NORM	0	0	0	0	6

Table 5.12 The best validation set detection result confusion matrices from FzCM3 at $C = 8$.

without PCA

Program output \ Desired output	ARCH	SPIC	CALC	CIRC	NORM
ARCH	5	0	0	0	1
SPIC	0	6	0	0	0
CALC	0	0	3	0	0
CIRC	1	0	0	2	0
NORM	0	0	0	0	6

with PCA

Program output \ Desired output	ARCH	SPIC	CALC	CIRC	NORM
ARCH	4	2	0	0	0
SPIC	0	6	0	0	0
CALC	0	0	2	0	1
CIRC	0	0	0	3	0
NORM	0	0	0	0	6

Table 5.13 The best validation set detection result confusion matrices from FzCM4 at $C = 8$.

without PCA

Program output \ Desired output	ARCH	SPIC	CALC	CIRC	NORM
ARCH	4	0	1	0	1
SPIC	0	6	0	0	0
CALC	0	0	3	0	0
CIRC	0	0	0	3	0
NORM	1	0	0	0	5

with PCA

Program output \ Desired output	ARCH	SPIC	CALC	CIRC	NORM
ARCH	3	2	0	1	0
SPIC	1	5	0	0	0
CALC	0	0	2	0	1
CIRC	0	1	0	2	0
NORM	0	1	0	0	5

Table 5.14 The best validation set detection result confusion matrices from FzCM5 at $C = 8$.

without PCA

Program output \ Desired output	ARCH	SPIC	CALC	CIRC	NORM
ARCH	5	0	0	0	1
SPIC	0	6	0	0	0
CALC	1	0	1	0	1
CIRC	0	0	0	3	0
NORM	0	0	0	0	6

with PCA

Program output \ Desired output	ARCH	SPIC	CALC	CIRC	NORM
ARCH	3	0	2	1	0
SPIC	0	6	0	0	0
CALC	0	0	1	0	2
CIRC	0	0	0	3	0
NORM	0	0	0	0	6

Table 5.15 The best validation set detection result confusion matrices from FzCM6 at $C = 8$.

without PCA

Program output \ Desired output	ARCH	SPIC	CALC	CIRC	NORM
ARCH	6	0	0	0	0
SPIC	0	6	0	0	0
CALC	1	0	2	0	0
CIRC	0	0	0	3	0
NORM	0	0	0	0	6

with PCA

Program output \ Desired output	ARCH	SPIC	CALC	CIRC	NORM
ARCH	6	0	0	0	0
SPIC	1	5	0	0	0
CALC	0	0	3	0	0
CIRC	0	0	0	3	0
NORM	0	0	0	0	6

Table 5.16 The best validation set detection results from GLCM feature sets.

N_g	Feature set	non PCA		PCA	
		RBF (σ)	ACC (%)	RBF (σ)	ACC (%)
4	GLCM1	0.25	70.83	2.00	75.00
	GLCM2	0.75	83.33	2.50	83.33
	GLCM3	0.50	83.33	1.50	87.50
	GLCM4	0.5	87.50	0.50	83.33
	GLCM5	1.0	91.67	2.00	87.50
	GLCM6	1.50	87.50	1.00	83.33
8	GLCM1	1.50	62.50	0.10	62.50
	GLCM2	0.50	75.00	1.00	83.33
	GLCM3	0.50	79.17	0.75	75.00
	GLCM4	2.50	95.83	0.25	75.00
	GLCM5	1.50	79.19	2.00	91.67
	GLCM6	2.00	100.00	1.50	91.67

Table 5.17 The best validation set detection result confusion matrices from GLCM1 at $N_g = 4$.

without PCA

Program output \ Desired output	ARCH	SPIC	CALC	CIRC	NORM
ARCH	5	0	0		1
SPIC	1	4	0	1	0
CALC	0	0	2	0	1
CIRC	0	0	0	3	0
NORM	0	0	0	0	6

with PCA

Program output \ Desired output	ARCH	SPIC	CALC	CIRC	NORM
ARCH	4	1	0	0	1
SPIC	2	3	0	1	0
CALC	1	0	2	0	0
CIRC	0	0	0	3	0
NORM	0	0	0	0	6

Table 5.18 The best validation set detection result confusion matrices from GLCM2 at $N_g = 4$.

without PCA

Program output \ Desired output	ARCH	SPIC	CALC	CIRC	NORM
ARCH	5	1	0	0	0
SPIC	0	5	1	0	0
CALC	0	0	3	0	0
CIRC	0	0	0	3	0
NORM	0	1	0	0	5

with PCA

Program output \ Desired output	ARCH	SPIC	CALC	CIRC	NORM
ARCH	6	0	0	0	0
SPIC	0	6	0	0	0
CALC	0	1	1	0	1
CIRC	0	0	0	3	0
NORM	0	0	0	0	6

Table 5.19 The best validation set detection result confusion matrices from GLCM3 at $N_g = 4$.

without PCA

Program output \ Desired output	ARCH	SPIC	CALC	CIRC	NORM
ARCH	6	0	0	0	0
SPIC	1	5	0	0	0
CALC	0	0	3	0	0
CIRC	0	0	0	3	0
NORM	0	0	0	0	6

with PCA

Program output \ Desired output	ARCH	SPIC	CALC	CIRC	NORM
ARCH	6	0	0	0	0
SPIC	0	6	0	0	0
CALC	0	0	1	0	2
CIRC	0	0	0	3	0
NORM	0	0	0	0	6

Table 5.20 The best validation set detection result confusion matrices from GLCM4 at $N_g = 4$.

without PCA

Program output \ Desired output	ARCH	SPIC	CALC	CIRC	NORM
ARCH	5	0	0	0	1
SPIC	0	6	0	0	0
CALC	1	0	2	0	0
CIRC	0	0	0	3	0
NORM	1	0	0	0	5

with PCA

Program output \ Desired output	ARCH	SPIC	CALC	CIRC	NORM
ARCH	6	0	0	0	0
SPIC	0	6	0	0	0
CALC	2	0	1	0	0
CIRC	0	0	0	3	0
NORM	2	0	0	0	4

Table 5.21 The best validation set detection result confusion matrix from GLCM5 at $N_g = 4$.

without PCA

Program output \ Desired output	ARCH	SPIC	CALC	CIRC	NORM
ARCH	5	1	0	0	0
SPIC	0	6	0	0	0
CALC	0	0	3	0	0
CIRC	0	0	0	3	0
NORM	1	0	0	0	5

with PCA

Program output \ Desired output	ARCH	SPIC	CALC	CIRC	NORM
ARCH	5	0	0	1	0
SPIC	0	4	0	0	2
CALC	0	0	3	0	0
CIRC	0	0	0	3	0
NORM	0	0	0	0	6

Table 5.22 The best validation set detection result confusion matrices from GLCM6 at $N_g = 4$.

without PCA

Program output \ Desired output	ARCH	SPIC	CALC	CIRC	NORM
ARCH	5	0	0	1	0
SPIC	0	6	0	0	0
CALC	1	0	2	0	0
CIRC	0	0	0	3	0
NORM	0	1	0	0	5

with PCA

Program output \ Desired output	ARCH	SPIC	CALC	CIRC	NORM
ARCH	6	0	0	0	0
SPIC	0	4	0	0	2
CALC	0	0	2	0	1
CIRC	0	0	0	3	0
NORM	0	0	0	1	5

Table 5.23 The best validation set detection result confusion matrices from GLCM1 at $N_g = 8$.

without PCA

Program output \ Desired output	ARCH	SPIC	CALC	CIRC	NORM
ARCH	6	0	0	0	0
SPIC	1	5	0	0	0
CALC	0	0	1	0	2
CIRC	0	0	0	3	0
NORM	1	0	0	0	5

with PCA

Program output \ Desired output	ARCH	SPIC	CALC	CIRC	NORM
ARCH	5	0	0	0	1
SPIC	0	6	0	0	0
CALC	0	0	3	0	0
CIRC	0	1	0	2	0
NORM	1	0	0	0	5

Table 5.24 The best validation set detection result confusion matrices from GLCM2 at $N_g = 8$.

without PCA

Program output \ Desired output	ARCH	SPIC	CALC	CIRC	NORM
ARCH	6	0	0	0	0
SPIC	0	6	0	0	0
CALC	1	0	2	0	0
CIRC	0	0	0	3	0
NORM	0	0	0	0	6

with PCA

Program output \ Desired output	ARCH	SPIC	CALC	CIRC	NORM
ARCH	6	0	0	0	0
SPIC	1	5	0	0	0
CALC	2	1	0	0	0
CIRC	2	0	0	0	1
NORM	0	0	0	0	6

Table 5.25 The best validation set detection result confusion matrices from GLCM3 at $N_g = 8$.

without PCA

Program output \ Desired output	ARCH	SPIC	CALC	CIRC	NORM
ARCH	5	0	0	0	1
SPIC	0	6	0	0	0
CALC	0	0	3	0	0
CIRC	1	0	0	2	0
NORM	0	0	0	0	6

with PCA

Program output \ Desired output	ARCH	SPIC	CALC	CIRC	NORM
ARCH	4	2	0	0	0
SPIC	0	6	0	0	0
CALC	0	0	2	0	1
CIRC	0	0	0	3	0
NORM	0	0	0	0	6

Table 5.26 The best validation set detection result confusion matrices from GLCM4 at $N_g = 8$.

without PCA

Program output \ Desired output	ARCH	SPIC	CALC	CIRC	NORM
ARCH	6	0	0	0	0
SPIC	0	6	0	0	0
CALC	0	0	3	0	0
CIRC	0	1	0	2	0
NORM	0	0	0	0	6

with PCA

Program output \ Desired output	ARCH	SPIC	CALC	CIRC	NORM
ARCH	5	0	0	0	1
SPIC	1	5	0	0	0
CALC	0	0	0	0	3
CIRC	0	1	0	2	0
NORM	0	0	0	0	6

Table 5.27 The best validation set detection result confusion matrix from GLCM5 at $N_g = 8$.

without PCA

Program output \ Desired output	ARCH	SPIC	CALC	CIRC	NORM
ARCH	5	0	1	0	0
SPIC	0	6	0	0	0
CALC	1	0	1	0	1
CIRC	0	1	0	2	0
NORM	1	0	0	0	5

with PCA

Program output \ Desired output	ARCH	SPIC	CALC	CIRC	NORM
ARCH	6	0	0	0	0
SPIC	0	6	0	0	0
CALC	2	0	1	0	0
CIRC	0	0	0	3	0
NORM	0	0	0	0	6

Table 5.28 The best validation set detection result confusion matrices from GLCM6 at $N_g = 8$.

without PCA

Program output \ Desired output	ARCH	SPIC	CALC	CIRC	NORM
ARCH	6	0	0	0	0
SPIC	0	6	0	0	0
CALC	0	0	3	0	0
CIRC	0	0	0	3	0
NORM	0	0	0	0	6

with PCA

Program output \ Desired output	ARCH	SPIC	CALC	CIRC	NORM
ARCH	5	1	0	0	0
SPIC	1	5	0	0	0
CALC	0	0	3	0	0
CIRC	0	0	0	3	0
NORM	0	0	0	0	6

In the testing process, we tested the system with the blind test data set. Since the size of the mammograms was 1024×1024, we scanned 64×64 pixel window with the step size of 16 pixels from top to bottom and left to right in order to generate features from FzCM6 at four clusters. We implemented the threshold (TH) to the output from each classifier. To generalize, each confidence was normalized using equation 5.3. The result from the system was put at the center of that window. Then, we combined each window with 8-connected neighborhood to generate the abnormal region. The region was assigned as TP when it overlapped with the ground truth. We also implemented the model that gave the second best result on the validation set, i.e., FzCM2 at 8 clusters. Similarly, for a comparison, we also implemented GLCM6 from 8 gray levels on the blind test data set. We also implemented GLCM6 at 8 gray levels with PCA. The examples of successful ARCH, SPIC, CALC, and CIRC detection from the feature set generated from FCOM are shown in figure 5.3 – 5.6. In these figure, our detection system can be recognizing the abnormalities using threshold values up to 0.5.

$$x' = \frac{x - Min(X)}{Max(X) - Min(X)}. \tag{5.3}$$

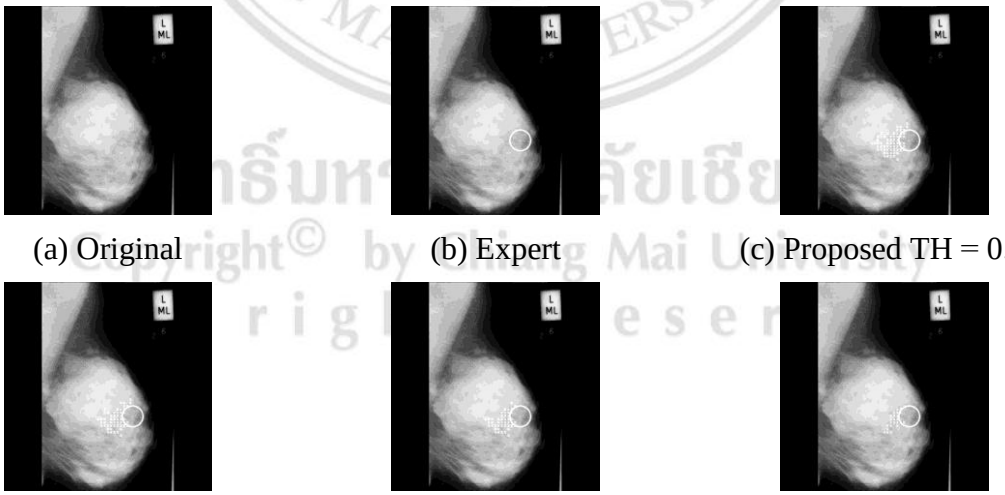

(a) Original (b) Expert (c) Proposed TH = 0.1

(d) Proposed TH = 0.2 (e) Proposed TH = 0.3 (f) Proposed TH = 0.5

Mdb163: ARCH

Figure 5.3 Example results of ARCH detection from FzCM4 at $C = 4$.

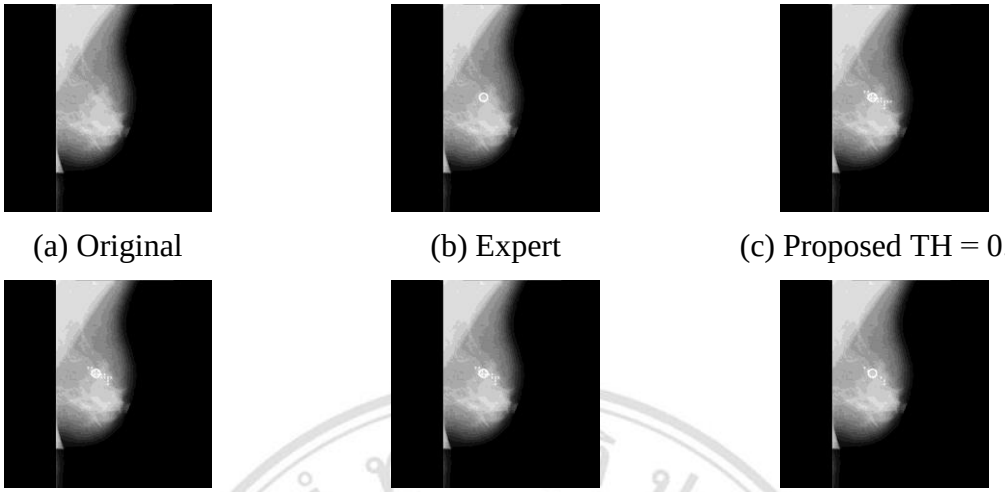

(a) Original (b) Expert (c) Proposed TH = 0.1

(d) Proposed TH = 0.2 (e) Proposed TH = 0.3 (f) Proposed TH = 0.5

Mdb207: SPIC

Figure 5.4 Example results of SPIC detection from FzCM4 at C = 4.

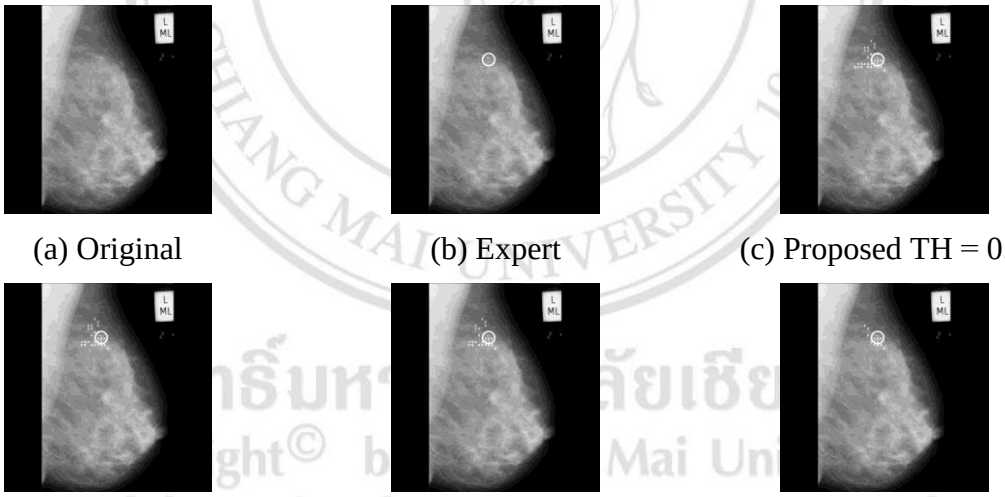

(a) Original (b) Expert (c) Proposed TH = 0.1

(d) Proposed TH = 0.2 (e) Proposed TH = 0.3 (f) Proposed TH = 0.5

Mdb219: CALC

Figure 5.5 Example results of CALC detection from FzCM4 at C = 4.

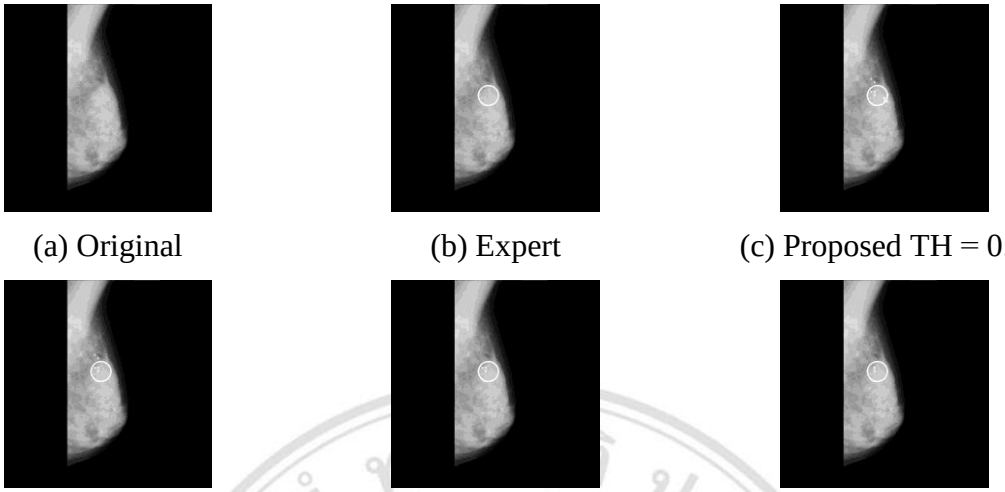

(a) Original (b) Expert (c) Proposed TH = 0.1

(d) Proposed TH = 0.2 (e) Proposed TH = 0.3 (f) Proposed TH = 0.5

Mdb017: CIRC

Figure 5.6 Example results of CIRC detection from FzCM4 at C = 4.

The best detection result for each class on blind test are shown in table 5.29. Table 5.30 to 5.33 show the details of detection result from FzCM2 at C = 4, FzCM3 at C = 8, GLCM2 at N_g = 8, and GLCM6 at N_g = 8, respectively.

Table 5.29 The best detection result on blind test data set.

The best detection for	Feature set	*Ng or C*	ACC (%)	False positive per image (FPI)
ARCH	FzCM3	8	100.00	8.28
	GLCM2	8	100.00	9.46
SPIC	FzCM2	4	90.00	13.72
	GLCM6	8	70.00	4.45
CALC	FzCM2	4	100.00	13.39
	GLCM6	8	89.47	10.81
CIRC	FzCM3	8	81.25	18.44
	GLCM2	8	68.75	6.78

Table 5.30 The detection result details from FzCM3 at C = 8.

Threshold	ARCH		SPIC		CALC		CIRC	
	ACC	FPI	ACC	FPI	ACC	FPI	ACC	FPI
0.10	100.00	14.70	90.00	15.40	89.47	18.22	81.25	18.44
0.15	100.00	14.45	80.00	14.87	89.47	17.57	81.25	18.06
0.20	100.00	14.15	80.00	14.40	89.47	16.64	81.25	17.24
0.25	100.00	13.66	80.00	13.50	89.47	15.36	81.25	15.87
0.30	100.00	13.02	80.00	12.78	89.47	13.83	68.75	14.19
0.35	100.00	12.06	70.00	11.78	78.95	12.25	62.50	12.23
0.40	100.00	10.83	70.00	10.64	78.95	10.48	56.25	10.06
0.45	100.00	9.58	70.00	9.42	73.68	8.50	43.75	8.07
0.50	100.00	8.28	70.00	7.78	73.68	6.78	43.75	6.21
0.55	77.78	6.82	60.00	6.50	63.16	5.02	43.75	4.51
0.60	66.67	5.73	60.00	5.06	63.16	3.44	37.50	3.18
0.65	55.56	4.30	50.00	3.62	57.89	2.33	37.50	2.35
0.70	55.56	3.05	30.00	2.58	31.58	1.56	25.00	1.57
0.75	44.44	2.02	30.00	1.66	10.53	0.89	25.00	0.98
0.80	11.11	1.29	10.00	0.98	10.53	0.50	18.75	0.60
0.85	11.11	0.71	10.00	0.51	5.26	0.24	6.25	0.27
0.90	11.11	0.34	0.00	0.24	0.00	0.08	0.00	0.09
0.95	0.00	0.10	0.00	0.06	0.00	0.02	0.00	0.05
1.00	0.00	0.00	0.00	0.00	0.00	0.00	0.00	0.00

Table 5.31 The detection result details from FzCM2 at C = 4.

Threshold	ARCH		SPIC		CALC		CIRC	
	ACC	FPI	ACC	FPI	ACC	FPI	ACC	FPI
0.10	100.00	16.28	90.00	16.75	100.00	13.39	62.50	11.06
0.15	88.89	15.18	90.00	16.21	94.74	12.98	56.25	9.68
0.20	88.89	14.07	90.00	15.25	94.74	12.37	56.25	8.47
0.25	88.89	12.74	90.00	13.72	89.47	11.75	50.00	7.39
0.30	77.78	11.17	80.00	12.22	89.47	11.04	37.50	6.22
0.35	77.78	9.65	70.00	10.68	84.21	9.94	31.25	5.24
0.40	77.78	8.31	70.00	8.94	84.21	8.74	31.25	4.23
0.45	77.78	7.03	70.00	7.16	84.21	7.66	31.25	3.39
0.50	44.44	5.72	60.00	5.56	73.68	6.36	31.25	2.58
0.55	44.44	4.65	60.00	4.33	63.16	5.02	25.00	1.90
0.60	44.44	3.66	50.00	3.29	57.89	3.89	18.75	1.42
0.65	33.33	2.74	40.00	2.43	57.89	2.82	18.75	1.01

Threshold	ARCH		SPIC		CALC		CIRC	
	ACC	FPI	ACC	FPI	ACC	FPI	ACC	FPI
0.70	11.11	1.97	40.00	1.62	47.37	1.88	12.50	0.77
0.75	0.00	1.33	20.00	1.11	47.37	1.16	6.25	0.52
0.80	0.00	0.81	20.00	0.74	42.11	0.68	0.00	0.33
0.85	0.00	0.51	10.00	0.41	42.11	0.35	0.00	0.21
0.90	0.00	0.26	10.00	0.24	26.32	0.17	0.00	0.14
0.95	0.00	0.07	0.00	0.10	5.26	0.04	0.00	0.04
1.00	0.00	0.00	0.00	0.00	0.00	0.00	0.00	0.00

Table 5.32 The detection result details from GLCM2 at N_g = 8.

Threshold	ARCH		SPIC		CALC		CIRC	
	ACC	FPI	ACC	FPI	ACC	FPI	ACC	FPI
0.10	100.00	9.30	60.00	6.37	89.47	9.99	68.75	6.78
0.15	100.00	9.33	50.00	5.96	89.47	9.69	68.75	6.23
0.20	100.00	9.42	40.00	5.50	89.47	9.34	68.75	5.79
0.25	100.00	9.57	40.00	4.91	89.47	8.98	56.25	5.31
0.30	100.00	9.47	40.00	4.35	84.21	8.60	56.25	4.83
0.35	88.89	9.33	40.00	3.68	78.95	8.23	56.25	4.40
0.40	88.89	8.94	30.00	3.17	78.95	7.56	56.25	3.97
0.45	88.89	8.56	30.00	2.70	73.68	7.08	56.25	3.49
0.50	88.89	7.67	30.00	2.32	68.42	6.52	50	3.01
0.55	88.89	7.06	20.00	1.89	63.16	5.89	31.25	2.61
0.60	77.78	5.92	20.00	1.55	63.16	5.34	31.25	2.16
0.65	44.44	4.87	20.00	1.23	52.63	4.60	31.25	1.79
0.70	44.44	3.81	10.00	0.95	52.63	3.91	25	1.43
0.75	33.33	2.82	10.00	0.73	42.11	3.05	18.75	1.07
0.80	33.33	2.03	10.00	0.51	36.84	2.16	18.75	0.82
0.85	22.22	1.24	10.00	0.32	26.32	1.35	18.75	0.55
0.90	0.00	0.67	0.00	0.19	0	0.72	12.5	0.34
0.95	0.00	0.23	0.00	0.07	0	0.24	6.25	0.17
1.00	0.00	0.00	0.00	0.00	0	0.00	0	0.00

Table 5.33 The detection result details from GLCM6 at N_g = 8.

Threshold	ARCH		SPIC		CALC		CIRC	
	ACC	FPI	ACC	FPI	ACC	FPI	ACC	FPI
0.10	88.89	11.28	70.00	6.36	89.47	10.81	68.75	10.04
0.15	88.89	11.19	70.00	6.23	89.47	10.83	68.75	9.60
0.20	88.89	11.20	70.00	6.03	84.21	10.60	68.75	9.18
0.25	88.89	10.93	70.00	5.65	78.95	10.32	68.75	8.46
0.30	77.78	10.67	70.00	5.31	73.68	9.81	56.25	7.73
0.35	77.78	10.47	70.00	4.93	68.42	8.93	43.75	7.16
0.40	77.78	10.18	70.00	4.45	68.42	7.97	43.75	6.78
0.45	77.78	9.70	60.00	4.03	57.89	7.10	43.75	6.20
0.50	77.78	9.12	40.00	3.54	57.89	6.18	37.5	5.56
0.55	55.56	8.49	40.00	3.07	52.63	5.27	31.25	4.82
0.60	55.56	7.61	30.00	2.59	26.32	4.41	18.75	4.11
0.65	55.56	6.45	30.00	2.08	21.05	3.64	12.5	3.45
0.70	44.44	5.23	20.00	1.62	15.79	2.89	6.25	2.73
0.75	33.33	4.10	20.00	1.22	5.26	2.19	6.25	2.19
0.80	22.22	2.96	10.00	0.86	5.26	1.64	6.25	1.66
0.85	22.22	1.84	10.00	0.55	5.26	1.08	6.25	1.16
0.90	11.11	0.92	0.00	0.29	0.00	0.62	6.25	0.67
0.95	0	0.30	0.00	0.11	0.00	0.28	0	0.32
1.00	0	0.00	0.00	0.00	0.00	0.00	0	0.00

From the results of blind test, the window size of 64×64 pixels was smaller than that of many abnormalities areas which might be the reason that there were many false positives per image. For example, some architectural distortion areas might be bigger than the window size, so the system might look at something similar in the signature library and classify those areas as ARCH instead of their corresponding true classes. One of the reasons that the system provides a wrong SPIC and CALC classification might be because sometimes there were calcification areas around a spiculated mass as shown in figure 5.7. There was only one model from FCOM that can detect SPIC in this figure. The results in the case are shown in figure 5.9. Or sometimes there was no spike boundary around the SPIC areas at all as shown in figure 5.8. As a result, the system might misclassify this area since there was no area similar to this kind of SPIC areas in the signature library. This might be also the reason why the system cannot detect some CIRC areas. Figure 5.10 shows an example of CIRC area that did not have a round

shape and was not similar to the ones in the signature library at all. In addition, we also scanned a window with step of 16, this may make the system miss some points which were important for the classification task.

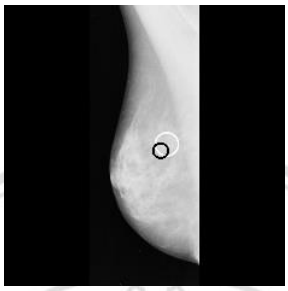

Figure 5.7 Example of CALC area (in black circle) that is overlapped with SPIC (in white circle).

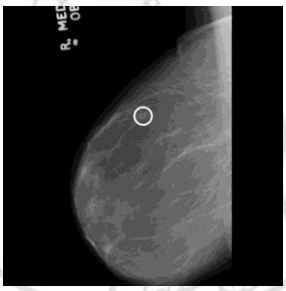

Figure 5.8 Example of SPIC (MDB190) area without spike.

In this case, our system can detected only using FzCM2 where C = 8. The detection results are shown in figure 5.9.

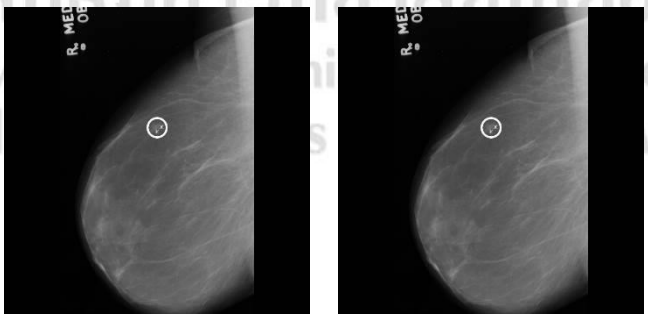

TH = 0.1 TH = 0.15

Figure 5.9 Results of SPIC dectection from MDB190.

Figure 5.10 Example of CIRC area that is misclssified.

From the experimental results, the proposed abnormalities mammogram detection system can be classifying all of ARCH, CALC, CIRC, and SPIC types. We found that the feature set computed from mean and standard deviation gave the higher average correct detection. From the characteristics of mammogram image, there were low gray levels distribution. Therefore, the feature sets extracted from four texture features i.e. contrast, correlation, energy, and homogeneity were suitable to use in detection system. We found out a two types of mammogram images that harder to diagnosis.

The first case was the mammogram images with the low global and local gray level distribution as shown figure 5.11. In this case, two of three types of this images were very smoothness as shown in (b) – (d). Hence, the texture features extracted from these images were also similar.

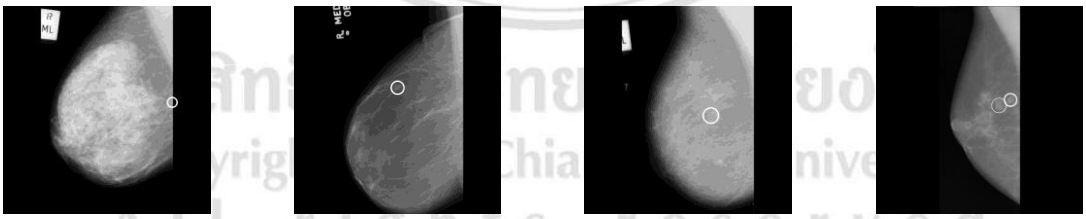

(a) ARCH: mdb126 (b) SPIC: mdb190 (c) CALC: mdb256 (d) CIRC: mdb059

Figure 5.11 An example for each class of abnormality types that least detected.

The second type was the high gray level distribution mammogram images in both of global and local area as shown in most false alarm images in figure 5.12. Identification of ROI or abnormality classes were not easier because the irregular pattern and the boundary of ROI were ambiguous both of shape and size.

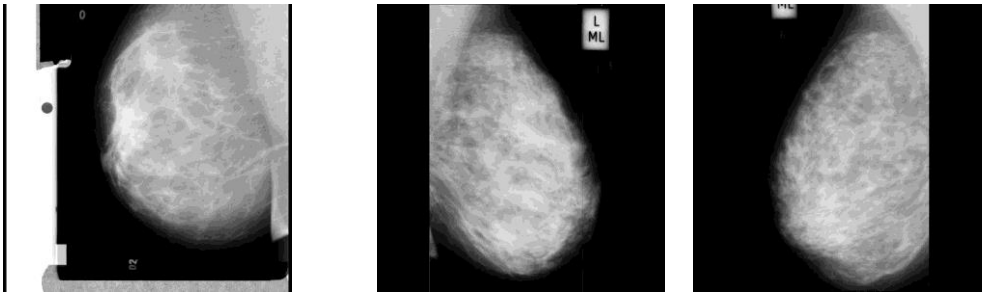

(a) ARCH and CALC: mdb280 (b) SPIC: mdb215 (c) CIRC: mdb130

Figure 5.12 An example of most created false alarm images.

5.3 Summary

This chapter proposed the breast abnormalities, i.e., calcification (CALC), well-defined/circumscribed masses (CIRC), speculated masses (SPIC), and architectural distortion (ARCH) detection system. We implemented multi-class support vector machine with one-versus-all strategy as a classifier on the FCOM to extract 14 features. We also compared the detection result with the same set of features extracted from the GLCM. The features extracted from our FCOM can yielded a better performance than those from the regular GLCM. The best blind test data set results for ARCH, SPIC, CALC, and CIRC detection from the feature set generated from our FCOM were 100% with 9.46 false positives per image (FPI), 90% with 13.72 FPI, 100% with 3.39 FPI, and 81.25% with 18 FPI, respectively. On the other hand, those for ARCH, SPIC, CALC, and CIRC detection from the feature set extracted from the GLCM were 100% with 9.46 FPI, 70% with 4.45 FPI, 89.47% with 10.81 FPI, and 68.75% with 6.78 FPI, respectively. There was no pre-processing or ROI selection in our system since we ran a sub-window across a mammogram and, in each sub-window, the FCOM was computed without any preprocessing. The generated features were then sent to the trained SVM to classify each sub-window.